AVS JVSTB Journal of Vacuum Science & Technology B

Comparative study of polycrystalline Ti, amorphous Ti, and multiamorphous Ti as a barrier film for Cu interconnect

Keng-Liang Ou, Ming-Sun Yu, Ray-Quen Hsu, and Ming-Hong Lin

Citation: Journal of Vacuum Science & Technology B **23**, 229 (2005); doi: 10.1116/1.1852466
View online: http://dx.doi.org/10.1116/1.1852466
View Table of Contents: http://scitation.aip.org/content/avs/journal/jvstb/23/1?ver=pdfcov
Published by the AVS: Science & Technology of Materials, Interfaces, and Processing

Articles you may be interested in

Improved barrier properties of ultrathin Ru film with TaN interlayer for copper metallization
Appl. Phys. Lett. **88**, 151912 (2006); 10.1063/1.2195112

Influence of N 2 O plasma treatment on microstructure and thermal stability of WN x barriers for Cu interconnection
J. Vac. Sci. Technol. B **22**, 993 (2004); 10.1116/1.1715087

Low leakage current Cu(Ti)/SiO 2 interconnection scheme with a self-formed TiO x diffusion barrier
Appl. Phys. Lett. **80**, 2678 (2002); 10.1063/1.1468913

Ti, TiN, and Ti/TiN thin films prepared by ion beam assisted deposition as diffusion barriers between Cu and Si
J. Vac. Sci. Technol. A **18**, 2312 (2000); 10.1116/1.1288942

Ultrathin and highly insulating amorphous- Ta 2 O 5 films formed on Ru/TiN/Ti /n + - Si substrates
Appl. Phys. Lett. **74**, 824 (1999); 10.1063/1.123380

Re-register for Table of Content Alerts

Create a profile.

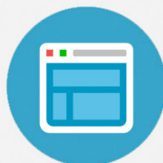

Sign up today!

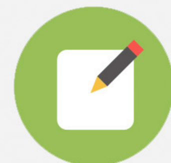

Redistribution subject to AVS license or copyright; see http://scitation.aip.org/termsconditions. Download to IP: 140.113.38.11 On: Thu, 01 May 2014 03:54:41

Comparative study of polycrystalline Ti, amorphous Ti, and multiamorphous Ti as a barrier film for Cu interconnect

Keng-Liang Ou
Graduate Institute of Oral Sciences, College of Oral Medicine, Taipei Medical University, 250 Wu-Hsing Street, 110 Taipei, Taiwan, Republic of China

Ming-Sun Yu
Haematology-Oncology Section, Department of Medicine, Veteran General Hospital, Kaohsiung 807, Taiwan, Republic of China

Ray-Quen Hsu
Institute and Department of Mechanical Engineering, National Chiao-Tung University, Hsinchu 300, Taiwan, Republic of China

Ming-Hong Lin[a)]
Department of Mechanical Engineering, National Kaohsiung University of Applied Sciences, Kaohsiung 807, Taiwan, Republic of China

(Received 13 May 2004; accepted 6 December 2004; published 14 January 2005)

Ultrathin (10 nm) Ti films with various structures were deposited by physical vapor deposition (PVD) and chemical vapor deposition (CVD) processes. CVD-Ti films with low-temperature (<500 °C) plasma-enhanced chemical vapor deposition using $TiCl_4$ and H_2 as reactants is an amorphous structure. This result is different from PVD-Ti films deposited by magnetron sputtering, which have a columnar structure. Ammonia plasma was further employed to post-treat the CVD-Ti barrier layer to improve barrier properties. An amorphous Ti(N,H) layer was formed on the surface of the CVD-Ti layer after ammonia plasma post-treatment. The resultant films had a bilayered amorphous Ti(N,H)/Ti structure. Furthermore, the effective resistivity of the resultant Ti(N,H)/Ti film decreased to 122 $\mu\Omega$ cm. The thermal stability of Cu/PVD-Ti/Si and Cu/CVD-Ti/Si contact systems was evaluated by thermal stressing at various annealing temperatures. For the Cu/PVD-Ti/Si, the highly copper titanium compound was formed after 450 °C annealing. The PVD Ti barrier failed initially due to the reaction of Cu and the Ti barrier, in which Cu atoms penetrated into the Si substrate after annealing at high temperature. However, no copper-titanium and copper-silicide compounds were found for amorphous Ti and plasma-treated Ti[Ti(N,H)/Ti] barriers, even after annealing at 500 and 600 °C, respectively. Improved barrier capability against Cu diffusion was found for the Ti(N,H)/Ti barrier layer because the Cu/Ti(N,H)/Ti/n^+-p junction diodes retained low leakage current densities even after annealing at 500 °C for 1 h. Ti(N,H)/Ti barrier layers present lengthened grain structures to effectively impede Cu diffusion, thus acting as much more effective barriers than conventional Ti and TiN films. © *2005 American Vacuum Society.*
[DOI: 10.1116/1.1852466]

I. INTRODUCTION

With the continuing increase in packing density of ultralarge scale integrated (ULSI) circuits, such as metal–oxide–semiconductor memory devices, geometrical dimensions (e.g., width of interconnections and isolation layers, junction depth, contact size) continue to decrease. However, this shrinkage causes various problems in device performance and reliability. In particular, problems with interconnections in copper metallization become quite serious, such as poor adhesion on dielectric films, degradation of shallow-junction characteristics by the alloy reaction between Cu and Si, and Cu migration.[1] Thus, the effective diffusion barriers are needed to prevent Cu diffusion and intermixing into silicon. Physical vapor deposited (PVD) Ti and TiN thin films are widely used as an adhesion layer and diffusion barrier in integrated-circuit devices because of their high thermal stability, excellent mechanical properties, and low electrical resistivity.[2–4] As the feature sizes of ULSI devices have shrunk, physical vapor deposition for such applications has been replaced by chemical vapor deposition (CVD), because of the increased conformability of the film as compared with PVD films.[2,5] CVD Ti and TiN layers can be deposited using a $TiCl_4$-based CVD process.[6–8] Nevertheless, this process requires high-temperature (>600 °C) substrates to achieve the depositions, which sometimes cause thermal damage to the deposited films and thermal diffusion of materials not suitable for devices. C49-$TiSi_2$ and TiN thin films are formed on the Si substrates in a conventional high-temperature $TiCl_4$-based Ti/TiN deposition process.[8] Moreover, deposited films are polycrystalline and provide inadequate protec-

[a)]Author to whom correspondence should be addressed; electronic mail: mhlin@cc.kuas.edu.tw

Redistribution subject to AVS license or copyright; see http://scitation.aip.org/termsconditions. Download to IP: 140.113.38.11 On: Thu, 01 May 2014 03:54:41

tion because grain boundaries may presumably serve as fast diffusion paths for copper. In this article, a low-temperature ($<500\ ^\circ C$) plasma-enhanced CVD (PECVD) was used to deposit ultrathin (10 nm) Ti films. Furthermore, *in situ* NH_3 plasma was employed to post-treat CVD-Ti films. Ti films by magnetron sputtering are compared with CVD-Ti and Ti(N,H)/Ti films. Properties of barrier layers were evaluated by electrical measurements and material analyses.

II. EXPERIMENTAL PROCEDURE

P-type (100)-oriented silicon wafers with resistivity of $5-10\ \Omega$ cm were used in our experiments. The Si wafers were cleaned in a dilute HF solution ($HF:H_2O=1:20$) for 2 min, and rinsed in de-ionized water before loading into metal-CVD system. Titanium films were deposited using an MRC PHOENIX 6 inch cluster tool. The Ti films (10 nm thick) were deposited by PECVD using $TiCl_4$ and H_2 as reactants. The substrate temperature was maintained at $490\ ^\circ C$ during Ti film deposition, and titanium films were deposited on 6 and 4 inch wafers at a power of 350 W and process pressure of 5 Torr after the base pressure was evacuated to below 5×10^{-7} Torr. Several wafers received an *in situ* plasma treatment after the deposition of titanium films. For the purpose of easy identification, the titanium films deposited by PVD and CVD and the ammonia plasma-treated titanium films were denoted as PVD-Ti, CVD-Ti, and CVD-Ti(N,H)/Ti, respectively. Copper films (300 nm thick) were then deposited on top of the barrier layers by sputtering. To evaluate the thermal stability, Cu/CVD-Ti/Si, Cu/PVD-Ti/Si, and Cu/Ti(N,H)/Ti/Si were annealed in N_2 ambient from 400 to 700 °C for 1 h. Scanning transmission electron microscopy (STEM) and grazing incidence x-ray diffractometry (GIXRD) were performed to determine the orientation of Ti-based barrier layers. Sheet resistance was performed to measure the conductive property of titanium film with and without treatments. To determine the capability of the barrier layer against copper diffusion, the microstructure was examined by using transmission electron microscopy (TEM). GIXRD was conducted for phase identification. The incident angle of x rays was fixed at three degrees. For electrical analyses, Cu/barrier/n^+-p junction diodes with conventional localized oxidation of silicon isolation were fabricated. The diode leakage current was measured by an HP4145B semiconductor parameter analyzer at a reverse bias of −5 V after annealing at various temperatures for 1 h.

III. RESULTS

Figure 1 plots the GIXRD pattern of as-deposited Ti film using various deposition processes. A strong Ti(002) peak appeared in a 10-nm-thick Ti film deposited by conventional sputtering. No obvious reflection peak is observed from the as-deposited Ti film using the PECVD process, revealing that the as-deposited Ti film has an amorphous structure, in contrast to PVD-Ti films. This result is similar to the results of Yang *et al.*[9] From the x-ray diffraction (XRD) pattern analyses of an NH_3 plasma-treated Ti film using the PECVD process, no obvious reflection peak is observed and the structure is amorphous. Figure 2 displays the STEM micrographs of as-deposited PVD-Ti films. The 10-nm-thick as-deposited PVD-Ti film has a columnar-like structure, as shown in the bright-field STEM image in Fig. 2, which has polycrystalline morphology with 30 nm grain sizes and obvious columnar-like structure. Figure 3 shows the cross-sectional STEM micrographs of Ti films with and without plasma treatment. The 10-nm-thick as-deposited CVD-Ti film has an amorphous structure, as shown in dark-field image in Fig. 3(a). The structure is quite different from that of PVD-Ti.[10,11] The chlorine concentration of as-deposited CVD-Ti films is about 1.78 at. % by energy-dispersive spectroscopy (EDS) analyses. Figure 3(b) shows a cross-sectional STEM micrograph of a CVD-Ti film post-treated with NH_3 plasma treatment. Its structure is observed to be a bilayer. NH_3 plasma treatment induces formation of another amorphous layer. Based on the x-ray photoelectron spectroscopy analyses (not shown), significant changes in the N 1*s* peak were observed for plasma-treated Ti films. With NH_3 plasma treatments, one peak at ~398 eV was found in the N 1*s* spectrum. It is attributed to $N^{\delta-}$, which is similar to the nitride ion. The presence of the N 1*s* peak clearly shows that the surface was nitrided by NH_3 plasma. This nitridation was also detected in tungsten film prepared by the reduction of WF_6 with N_2 in

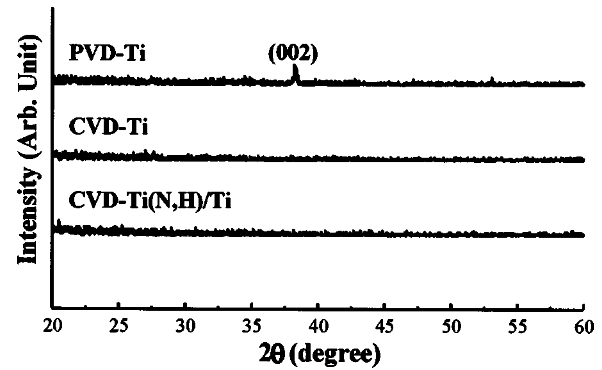

FIG. 1. X-ray diffraction pattern of as-deposited PVD-Ti, CVD-Ti, and Ti(N,H)/Ti films.

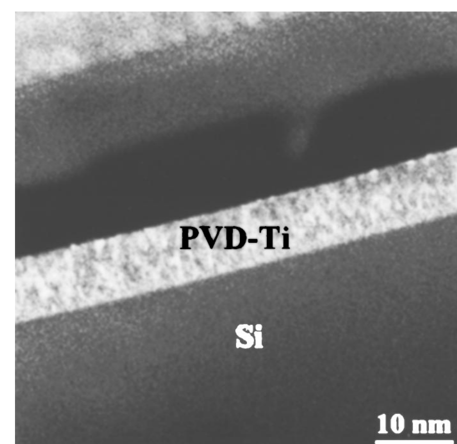

FIG. 2. Cross-sectional STEM micrographs of PVD-Ti.

Redistribution subject to AVS license or copyright; see http://scitation.aip.org/termsconditions. Download to IP: 140.113.38.11 On: Thu, 01 May 2014 03:54:41

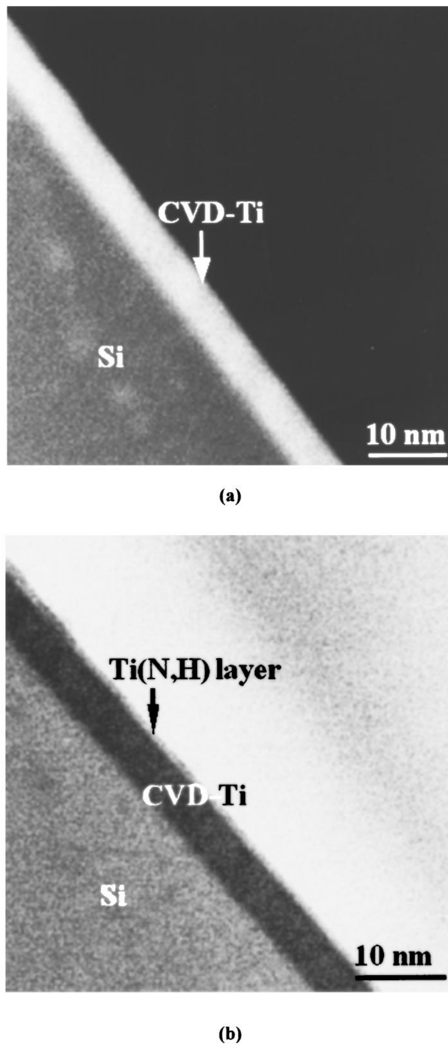

FIG. 3. Cross-sectional STEM micrographs of (a) CVD-Ti and (b) NH_3 plasma-treated Ti films.

nitrogen gas.[12] In addition, a lower Cl concentration of 0.33 at. % is detected on the surface of the NH_3 plasma-treated Ti film by EDS analyses. NH_3 plasma treatment also enhances the nitrogen incorporation to a depth of 1 nm. A high density of excited and unstable species, such as ions and radicals, is produced in the plasma, which constitutes a powerful reactive atmosphere. Moreover, because of their acceleration in the plasma sheath, the ionic species impinging on the surface have some kinetic energy, which enhances the activation of surface reactions. Figure 4 plots the electrical resistivity of the Ti(N,H)/Ti film as a function of plasma-treatment time. The resistivity of the as-deposited CVD-Ti film is about 338 $\mu\Omega$ cm. High resistivity is attributed to low deposition temperature. Suzuki *et al.* reported that a higher deposition temperature could reduce Cl concentration in conventional CVD-TiN film due to enhanced dissociation and reaction.[13] Resistivity decreases abruptly after NH_3 plasma treatment for 2 min because of the reduction of Cl concentration in the film. NH_3 plasma treatment is useful to reduce chlorine concentration. The resistivity decreased to

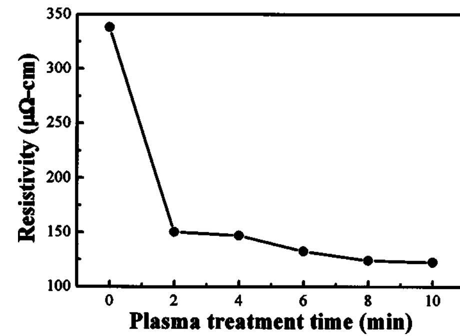

FIG. 4. Resistivity of Ti(N,H)/Ti film as a function of NH_3 plasma-treatment time.

122 $\mu\Omega$ cm for CVD-Ti film with NH_3 plasma treatment for 10 min. The resistivity is lower than that of conventional CVD-Ti/TiN films deposited at higher temperature. Mei *et al.* reported that effective resistivity of CVD-$TiSi_2$/TiN films decreased from 200 to 133 $\mu\Omega$ cm after NH_3 plasma treatment for 5 min.[14]

Figure 5 shows the variations in sheet resistance of Cu/barrier/Si after annealing at various temperatures. The variation in the sheet resistance is designated as the ratio of (R–Ro) to Ro, where Ro and R denote the sheet resistance of the as-deposited sample and R is the sheet resistance of the annealed sample. The result reflects the existence of interactions between layers. It is to be noted that the sheet resistance of the PVD-Ti barrier increases with the increase of annealing temperatures. However, sheet resistance of CVD-Ti and Ti(N,H)/Ti barriers initially decreases by annealing at 500 °C, which is caused by the decrease of Cl impurity density and grain growth in the Cu film. The sheet resistance of the Cu/CVD-Ti/Si increases after annealing at 600 °C, and the color of the sample changed to gray, which indicates that a significant reaction occurred between the layers. However, this phenomenon is not observed for Cu/Ti(N,H)/Ti/Si. This result indicates that there is no compound silicide formed when the sample is annealed up to 650 °C. It is obvious that CVD-Ti barrier films with post-treatment possess higher thermal stability than an as-sputtered Ti barrier film, and NH_3 plasma-treated Ti barrier film possesses the best thermal stability.

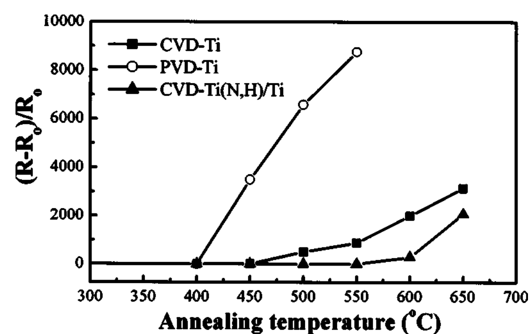

FIG. 5. Variation in sheet resistance of Cu/barrier/Si as a function of annealing temperature.

Redistribution subject to AVS license or copyright; see http://scitation.aip.org/termsconditions. Download to IP: 140.113.38.11 On: Thu, 01 May 2014 03:54:41

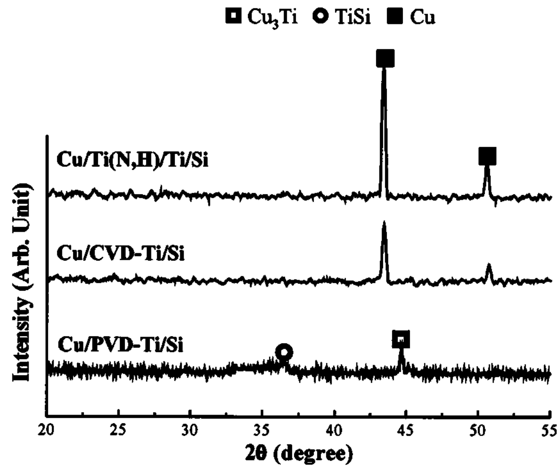

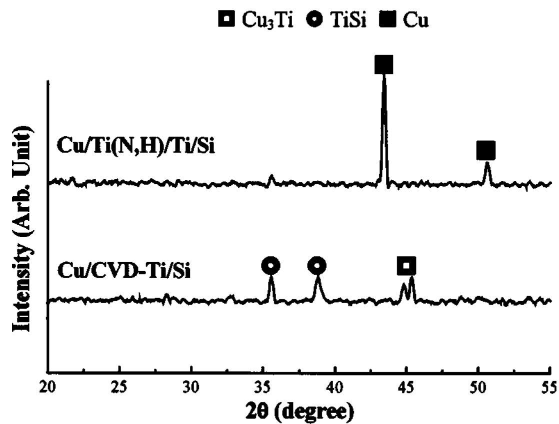

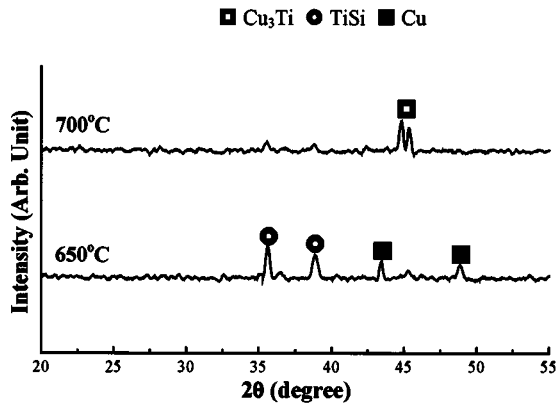

FIG. 6. XRD spectra of Cu/barrier/Si samples after annealing at (a) 500, (b) 600, and (c) 650 and 700 °C, respectively.

The formation of compounds at the interfaces during annealing was investigated by XRD analyses. The XRD patterns are shown in Fig. 6. Figure 6(a) shows the XRD patterns after annealing at 500 °C. Strong Cu(111) and weak Cu(200) peaks are observed in annealed Cu/CVD-Ti/Si and Cu/Ti(N,H)/Ti/Si samples, implying that the Cu films prefer the ⟨111⟩ crystal orientation. Cu with a high ⟨111⟩ texture

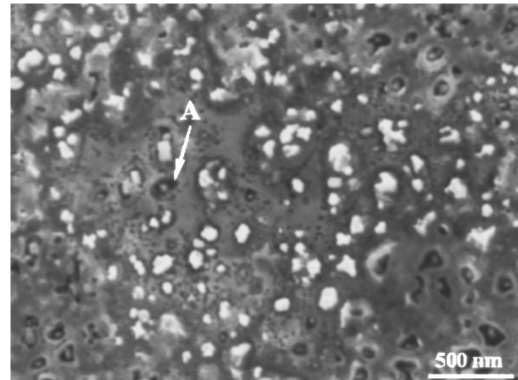

FIG. 7. SEM micrograph of 500 °C-annealed Cu/PVD-Ti/Si sample. Cu film is stripped after annealing.

has been reported to exhibit higher electromigration resistance.[15] The diffraction peaks of Ti(002) and Cu(111) clearly disappear and the Cu_3Ti phase appears for a Cu/PVD-Ti/Si sample annealed at 500 °C for 1 h. These results show that the interdiffusion of Cu and Ti induces the formation of Cu–Ti and Ti–Si compounds after 500 °C annealing. It is to be recognized that fine grains inherent in the thin films may lead to dominate grain-boundary diffusion after high-temperature annealing. Copper reacted with Si, and Cu–Si compounds were formed after annealing at 500 °C. This result induced the increase of sheet resistance. However, the Cu–Ti compounds are not observed in Cu/CVD-Ti/Si and Cu/Ti(N,H)/Ti/Si samples after annealing at 500 °C for 1 h. These results show that nitrogen incorporation in the amorphous Ti film can suppress the formation of Cu–Ti compounds. Figure 6(b) shows XRD patterns of the Cu/CVD-Ti/Si and Cu/Ti(N,H)/Ti/Si samples after annealing at 600 °C for 1 h. Strong Cu_3Ti and TiSi peaks are observed for the annealed Cu/CVD-Ti/Si sample. Strong Cu(111), weak Cu (200), and TiSi peaks are found in the XRD spectrum of the annealed Cu/Ti(N,H)/Ti/Si sample. The intensity of the TiSi peak is lower. Neither Cu–Si nor Cu–Ti compounds are observed after annealing at 600 °C. The results indicate that the Ti(N,H)/Ti barrier is more effective in preventing Cu diffusion than the CVD-Ti barrier. Figure 6(c) shows XRD patterns of the Ti(N,H)/Ti samples after annealing at 650 and 700 °C. The intensity of the TiSi peak clearly increases after annealing at 650 °C. It reveals that annealing causes the development of Ti(N,H)/Ti crystals. Obvious Cu_3Ti phases are found for Cu/Ti(N,H)/Ti/Si samples annealed at 700 °C for 1 h. The appearance of a reflection peak with a sharp intensity of Cu_3Ti phase indicates the start of the solid-phase reaction, probably at the interface of Cu/Ti. Scanning electron microscopy (SEM) was performed to investigate the surface morphologies after thermal annealing for further analyzing thermal stability. Protrusions or precipitates are observed on the surface after annealing at the temperature at which an abrupt increase of sheet resistance occurs. Figure 7 shows the SEM micrograph of the sample with a PVD-Ti barrier layer after annealing at 500 °C for 1 h. Copper film is stripped by

Redistribution subject to AVS license or copyright; see http://scitation.aip.org/termsconditions. Download to IP: 140.113.38.11 On: Thu, 01 May 2014 03:54:41

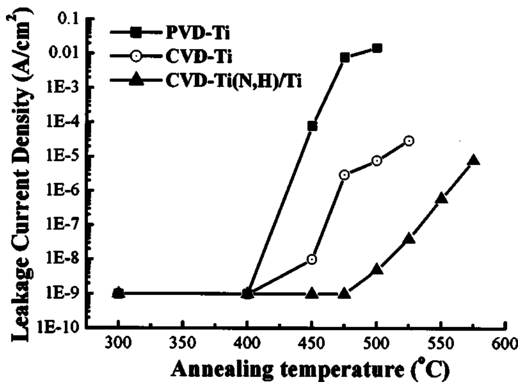

FIG. 8. Variation in leakage current density of Cu/barrier/Si as a function of annealing temperature.

wet solution before SEM analyses. It reveals local defect sites, as denoted by region A in Fig. 7. EDS is further employed to analyze the chemical compositions in region A. The concentrations of copper and titanium are 62.25 and 37.75 at. %, respectively. It reveals that Cu-rich defects form in local sites such as region A. It reveals that copper will penetrate and react with the PVD-Ti barrier layer during annealing at 500 °C. The formation of Cu–Ti compounds will promote Cu diffusion via a Ti-based barrier.

Junction leakage current measurements were conducted to investigate the effect of barrier treatment on Cu diffusion. The barrier performance of PVD-Ti, CVD-Ti, and Ti(N,H)/Ti films were investigated by measuring leakage current densities of Cu/barrier/n^+-p junction diodes after thermal stressing, and are shown in Fig. 8. The diode is defined as a failure when the measured current density is larger than 10^{-6} A/cm^2. Figure 8 plots the statistical distributions of leakage current densities of Cu/barrier/n^+-p junction diodes annealed at various temperatures. Cu/PVD-Ti/n^+-p junction diodes retain low leakage current densities up to annealing at 400 °C for 1 h. However, large leakage current densities in the range of 10^{-4} A/cm^2 are found after annealing at 450 °C. Improved barrier capability is found for the amorphous CVD-Ti barrier layer because the diodes retain low leakage current densities, even after annealing at 450 °C for 1 h. However, the improvement of the barrier capability is limited. As plasma treatment was performed, multilayered Ti(N,H)/Ti barrier was formed. The Cu/Ti(N,H)/Ti/n^+-p diodes retained better electrical integrity after annealing at 550 °C with lower leakage current densities (less than 10^{-6} A/cm^2). The Ti(N,H)/Ti films possess much better barrier performance than PVD-Ti and CVD-Ti barrier films. The barrier capability of CVD-Ti films is much better than conventional Ti and TiN layers reported in the literature. Ahrens *et al.* reported that most copper-contacted diodes with 10–100-nm-thick sputtered TiN barriers showed high leakage currents after annealing at 450 °C.[16] Poor barrier performance of the conventional Ti and TiN film is attributed to formation of columnar structure. This columnar structure is problematic for barrier applications because of intergranular voids, which provide diffusion paths. The microstructure within the barrier layer has been reported to strongly affect the barrier performance because Cu diffuses through fast diffusion paths such as grain boundaries within the barrier layer. Improved barrier performance of Ti(N,H)/Ti layers is ascribed to a nitridation effect and the formation of a multilayered amorphous structure. A multilayered and nanostructured amorphous diffusion barrier more effectively prevents Cu diffusion than does the polycrystalline barrier, because the amorphous film does not have large-angle grain boundaries at which most atomic diffusion typically occurs.[16]

IV. DISCUSSION

Based on the results of sheet resistance measurements, reversed leakage current density, and XRD analyses, we found that a difference of failure mechanism exists among PVD-Ti, CVD-Ti, and Ti(N,H)/Ti barriers. Figure 9 shows cross-sectional TEM micrographs of annealed Cu/PVD-Ti/n^+-p, Cu/CVD-Ti/n^+-p, and Cu/Ti(N,H)/Ti/n^+-p at various annealing temperatures for 1 h. As shown in Fig. 9(a), the copper spiking phenomenon of the interface is clearly observed. This indicates the degradation of the PVD-Ti barrier after annealing at 450 °C. Based on XRD results, the degradation of the Ti barrier is attributed to the diffusion of Cu into the Si substrate through the copper-titanium compound layer and/or diffusion from the Ti grain boundaries. Copper silicide is clearly formed. However, this phenomenon is also similarly observed in the Cu/CVD-Ti/n^+-p system after 600 °C annealing, as shown in Fig. 9(b). Figure 9(c) shows the cross-sectional TEM image of the Cu/Ti(N,H)/Ti/n^+-p sample after annealing at 600 °C for 1 h. An amorphous layer exists between the Cu- and Ti-based barrier layer. No Cu–Ti compounds can be found at the interface, which shows excellent barrier properties. This observation is in agreement with XRD results. The corresponding high-resolution TEM image of the annealed Cu/Ti(N,H)/Ti/n^+-p sample is shown in Fig. 9(d). It is obvious that the amorphous layer remained, even through high-temperature annealing. These investigations of cross-sectional TEM are in agreement with the XRD results, which indicate the diffusion of Cu atoms through the amorphous layer and the formation of compounds containing Cu, Ti, and Si are the main causes of failure for the Cu/Ti(N,H)/Ti/Si system. Furthermore, as Cu/Ti(N,H)/Ti/n^+-p junction diodes were annealed up to 550 °C, Ti(N,H)/Ti functions as an effective barrier against Cu diffusion for the sheet-resistance measurement, whereas most of samples failed in the junction leakage evaluation. Results suggest that junction leakage is more suitable for evaluating the barrier capability of Ti(N,H)/Ti films on the Cu/Ti(N,H)/Ti/n^+-p junction diodes than the variation of sheet resistance.

The cross sections of the interfacial structures of Cu/PVD-Ti/Si, Cu/CVD-Ti/Si, and Cu/Ti(N,H)/Ti/Si before and after annealing are shown schematically in Fig. 10. Cu films on PVD-Ti, CVD-Ti, and Ti(N,H)/Ti barriers have preferred {111} orientation. The as-deposited PVD-Ti barrier has a columnar structure, as shown in Fig. 10(a). After an-

Redistribution subject to AVS license or copyright; see http://scitation.aip.org/termsconditions. Download to IP: 140.113.38.11 On: Thu, 01 May 2014 03:54:41

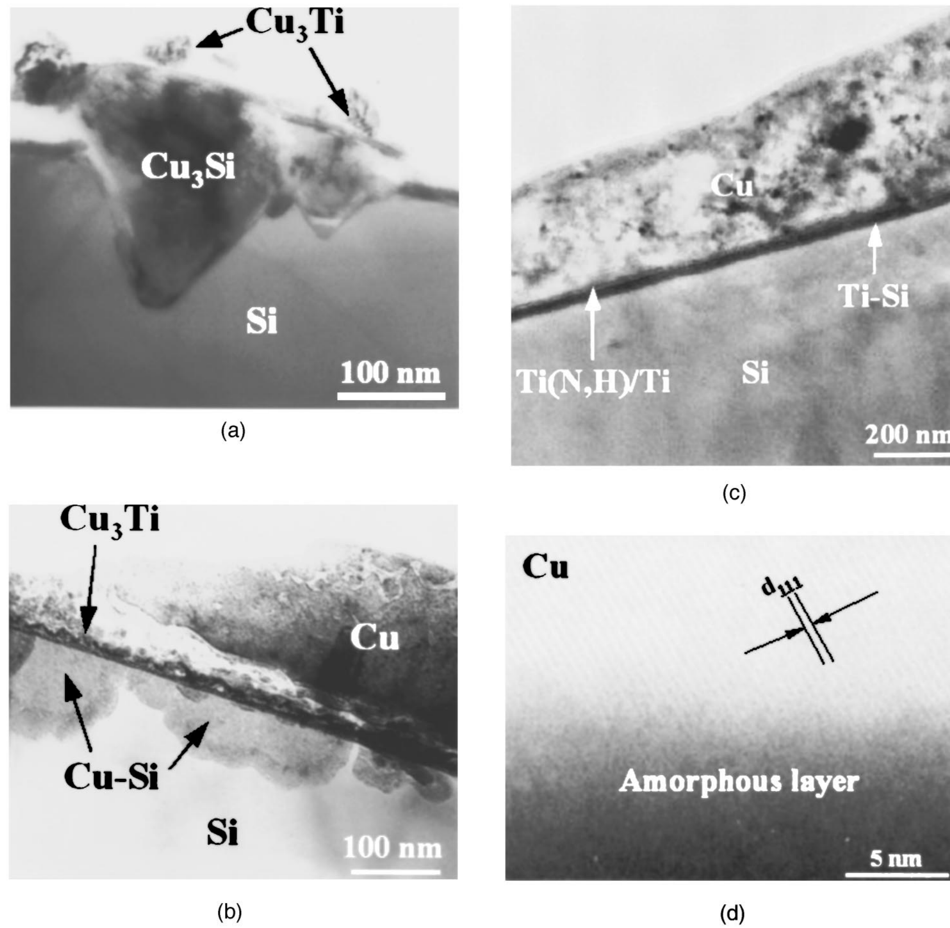

FIG. 9. Cross-sectional TEM micrographs of (a) 450 °C-annealed Cu/PVD-Ti/n^+-p, (b) 450 °C-annealed Cu/CVD-Ti/n^+-p, (c) 600 °C-annealed Cu/Ti(N,H)/Ti/n^+-p, and (d) high-resolution TEM image of the annealed Cu/Ti(N,H)/Ti/n^+-p.

nealing at 450 °C for 1 h, the observation of copper titanium Cu_3Ti and copper spiking indicates barrier degradation. After annealing at 500 °C, in addition to more Cu_3Ti and copper spiking, Cu–Si also can be formed and further degrades the barrier. The mechanism by which the barrier fails is the motion of Cu through the columnar Ti to form Cu_3Ti and spiking. The similar result, as shown in Fig. 10(b), is observed from the amorphous CVD-Ti barrier. The barrier capability of Ti films against Cu diffusion can be enhanced by incorporating nitrogen in Ti films by the plasma technique. The microstructure of the plasma-treated Ti films can be changed from a single amorphous layer to a bilayer amorphous structure. The Ti(N,H)/Ti film has an amorphous-like structure and can function as a more-effective barrier against Cu diffusion.[9,16] The CVD-Ti barrier with *in situ* NH_3 plasma treatment has an amorphous Ti(N,H)/Ti structure, as shown in Fig. 10(c). The formation of a thin amorphous Ti(N,H)/Ti layer on the surface of the Ti film can be observed after the ammonia plasma treatment. This Ti(N,H)/Ti barrier can effectively prevent the Cu/Si and Cu/Ti reaction. An additional amorphous layer can be

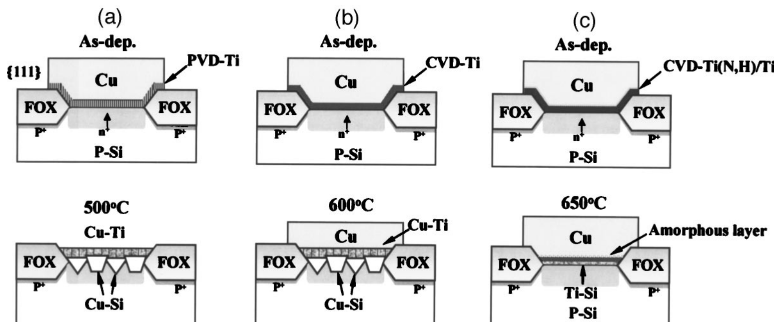

FIG. 10. Schematic illustrations of the microstructure of (a) Cu/PVD-Ti/n^+-p, (b) Cu/CVD-Ti/n^+-p and, (c) Cu/Ti(N,H)/Ti/n^+-p samples before and after annealing.

Redistribution subject to AVS license or copyright; see http://scitation.aip.org/termsconditions. Download to IP: 140.113.38.11 On: Thu, 01 May 2014 03:54:41

formed between the Cu and barrier layer after annealing at 600 °C for 1 h. This barrier can retain its integrity even after annealing at 650 °C for 1 h. Copper-titanium compounds and titanium silicides were observed, instead of copper silicides, in this study. An amorphous Ti(N,H) layer was formed on the surface of the CVD-Ti layer after ammonia plasma post-treatment. It would alleviate the Cu diffusion and hence enhance barrier stability and restrain copper diffusion. High thermal stability of Cu/Ti(N,H)/Ti/Si is obtained.

V. CONCLUSION

In summary, a multilayered amorphous Ti(N,H)/Ti barrier layer was prepared and successfully applied to Cu metallization. Ultrathin (10 nm) Ti(N,H)/Ti barrier films were prepared by low-temperature (<500 °C) plasma-enhanced chemical vapor deposition using $TiCl_4$ and H_2 as reactants and following *in situ* ammonia plasma treatment. NH_3 plasma treatment is useful to reduce chlorine concentration and enhance nitrogen incorporation. An amorphous Ti(N,H) layer was formed on the surface of the Ti layer after ammonia plasma post-treatment. The chlorine concentration decreased from 1.78 to 0.33 at. %. Low effective resistivity of 122 $\mu\Omega$ cm was obtained for resultant Ti(N,H)/Ti film due to reduction of chlorine concentration. In addition, improved barrier capability against Cu diffusion is found for the Ti(N,H)/Ti barrier layer because the Cu/Ti(N,H)/Ti/n^+-p junction diodes retain low leakage current densities, even after annealing at 500 °C for 1 h. The Ti(N,H)/Ti barrier layer presents a multilayered and nanostructured amorphous structure that is more effective in preventing Cu diffusion than the polycrystalline barrier, because the nanostructured amorphous film does not have large-angle grain boundaries at which most atomic diffusion typically occurs.

ACKNOWLEDGMENTS

The work was financially supported by the National Science Council of the Republic of China under Contract Nos. NSC 92-2212-E-009-028 and NSC-93-2320-B-038-034.

[1]T. Nitta, T. Hoshi, S. Sakai, K. Sakaibara, S. Imai, and T. Shibata, J. Electrochem. Soc. **140**, 1131 (1993).
[2]J. D. Mcbrayer, R. M. Swanson, and T. W. Sigmon, J. Electrochem. Soc. **123**, 1242 (1986).
[3]T. Kouno, H. Niwa, and M. Yamada, J. Electrochem. Soc. **145**, 2614 (1998).
[4]J. Baumann, T. Werner, A. Ehrlich, M. Rennau, Ch. Kaufmann, and T. Gessner, Microelectron. Eng. **37/38**, 221 (1997).
[5]K. Holloway and P. M. Fryer, J. Appl. Phys. **71**, 5433 (1992).
[6]X. Sun, E. Kolawa, J. S. Chen, J. S. Reid, and M. A. Nicolet, Thin Solid Films **236**, 347 (1993).
[7]*ASM Handbook* (ASM, New York, 1992), Vol. 3.
[8]T. Okamoto, M. Shimizu, A. Ohsaki, Y. Mashiko, K. Tsukamoto, T. Matsukawa, and S. Nagao, J. Appl. Phys. **62**, 4465 (1987).
[9]W. L. Yang, W. F. Wu, D. G. Lin, C. C. Wu, and K. L. Ou, Solid-State Electron. **45**, 149 (2001).
[10]K. H. Min, K. C. Chun, and K. B. Kim, J. Vac. Sci. Technol. B **14**, 3263 (1996).
[11]G. S. Chen and S. T. Chen, J. Appl. Phys. **87**, 8473 (2000).
[12]T. Nakajima, K. Watanable, and N. Watanabe, J. Electrochem. Soc. **134**, 3175 (1987).
[13]T. Suzuki, T. Ohba, Y. Furumura, and H. Tsutikawa, in *Proceedings of the 10th International VLSI Multilevel Interconnection Conference*, Santa Clara, June 1993, p. 418.
[14]Y. J. Mei *et al.*, Thin Solid Films **308/309**, 594 (1997).
[15]K. L. Ou, W. F. Wu, C. P. Chou, C. S. Chiou, and C. C. Wu, J. Vac. Sci. Technol. B **20**, 2154 (2002).
[16]C. Ahrens, R. Ferretti, G. Friese, and J. O. Weidner, Microelectron. Eng. **37/38**, 221 (1997).

Redistribution subject to AVS license or copyright; see http://scitation.aip.org/termsconditions. Download to IP: 140.113.38.11 On: Thu, 01 May 2014 03:54:41